ACS OMEGA

http://pubs.acs.org/journal/acsodf

Article

Adsorption Equilibria, Kinetics, and Column Dynamics of L-Tryptophan on Mixed-Mode Resin HD-1

Pengfei Jiao,* Xin Zhang, Yuping Wei, and Yiyan Meng

Cite This: *ACS Omega* 2022, 7, 9614−9621

Read Online

ACCESS | Metrics & More | Article Recommendations

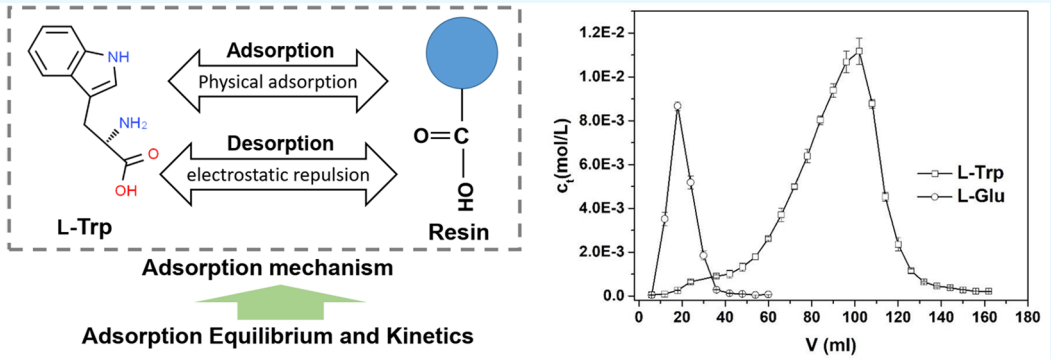

ABSTRACT: The adsorption amount and selectivity of L-tryptophan (L-Trp) on the hydrophobic interaction and ion exchange mixed-mode chromatography medium HD-1 were studied as well as the salt resistance of the resin via adsorption equilibrium experiments. The adsorption mechanisms of L-Trp were illuminated by combining adsorption equilibria and a kinetics analysis. The separation effect was studied by dynamic separation experiments in a fixed-bed. The results indicate that an increase of the concentration proportion of L-Trp zwitterion benefits the adsorption of L-Trp. The resin shows a high adsorption selectivity for L-Trp at different pH values. The adsorption amount of L-Trp is not affected significantly by NaCl. Various groups play a role in the adsorption of L-Trp. An adsorption energy lower than 8 kJ/mol indicates that the adsorption of L-Trp is mainly based on non-electrostatic interactions, with an electrostatic interaction as a supplement. The adsorption equilibrium model considering the dissociation equilibrium of the resin and L-Trp proposed in this work can simulate the adsorption equilibrium data of L-Trp at different pH values as well. The mass transfer rate of L-Trp is controlled by intraparticle and liquid film diffusion simultaneously. The fixed-bed packed with resin HD-1 can separate L-Trp with the purity of L-Trp higher than 99%, recovery rate higher than 95%, and concentration of 4.69×10^{-3} mol/L.

1. INTRODUCTION

L-Tryptophan (L-Trp) is one of the essential amino acids for humans and animals. L-Trp has been widely used in food, pharmaceutical, and feed additives industries.[1−3] The preparation methods of L-Trp include hydrolysis of protein,[4] chemical synthesis,[5] microbiological fermentation,[6−8] and so on. However, the first two methods have been eliminated because of the long production period and complex process. Production of L-Trp by microbiological fermentation has the advantages of low production cost and high output. Therefore, it has been the most commonly used industrial production method for L-Trp.[9] The complex component in the fermentation broth leads to the separation and purification of L-Trp being one of the keys to the industrial production of L-Trp. After a pretreatment for removing impurities such as the microbial cell, proteins, and pigments, the fermentation broth of L-Trp also contains soluble salts (mainly NaCl and NH_4SO_4) and other amino acids (mainly L-glutamic acid (L-Glu)).[10]

The separation methods of L-Trp mainly include organic solvent extraction,[11] crystallization,[12] membrane separation,[13] ion exchange,[14−16] and physical adsorption.[10,17] Ion exchange is the widely used method for L-Trp separation because of the simple and inexpensive operation process. Many researchers have reported separations of L-Trp using strong acid cation exchange resins. Xie et al. studied the adsorption equilibria and kinetics performances of L-Trp on strong acid cation exchange

Received: December 9, 2021
Accepted: February 28, 2022
Published: March 9, 2022

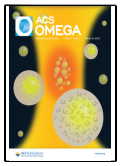

https://doi.org/10.1021/acsomega.1c06960
ACS Omega 2022, 7, 9614−9621

resin 001 × 7.[14] It was found that L-Trp was adsorbed on the resin based on a proton transfer reaction and ion exchange. Luo et al. studied the adsorption breakthrough and elution processes of L-Trp on the strong acid cation exchange resin HZ-001.[15] The adsorption breakthrough curves were predicted by Adams-Bohard, Wolborska, Thomas, and Yoon-Nelson models very well. However, the ion exchange capacity of the ion exchangers was reduced by lots of soluble salt in the fermentation broth of L-Trp. In our previous work, the separation of L-Trp by the weakly polar hyper-cross-linked adsorption resin XDA-200 was studied.[10,17] The resin shows a high separation resolution to L-Trp from L-Glu, which is the main purity in the pretreated fermentation broth of L-Trp except for the soluble salts. The elution chromatographic peak of L-Trp trailed significantly due to the strong affinity between the resin XDA-200 and L-Trp. Therefore, developing new efficient separation and purification methods is an important way to improve the efficiency and reduce cost for L-Trp production.

Mixed-mode chromatography is a new chromatography separation technology developed in recent years. The adsorbents used in the separation technology can adsorb target compounds including proteins and nucleotides via two or more interactions including hydrophobic interaction, electrostatic interactions, and hydrogen bonding.[18] The L-Trp molecule contains a hydrophobic indole group. Hydrophobic interaction/ion exchange mixed-mode adsorbents can adsorb L-Trp based on physical adsorption forces including a hydrophobic interaction, van der Waals force, and hydrogen bonding at an appropriate solution pH. Under the circumstances, the adsorption of L-Glu and soluble salts on the adsorbents can be avoided. A high adsorption selectivity of the adsorbents to L-Trp can be expected. L-Trp adsorbed on the adsorbents can be eluted easily based on the electrostatic repulsion by adjusting the pH of the eluent appropriately. Therefore, the efficient adsorption and elution of L-Trp can be realized by a reasonable pH adjustment of the feed solution and eluent. In summary, hydrophobic interaction/ion exchange mixed-mode chromatography is one of the efficient separation methods for L-Trp.

In this work, the hydrophobic interaction/ion exchange mixed-mode resin HD-1 was used to separate L-Trp from its pretreated fermentation broth. The adsorption equilibria, kinetics, and column dynamics were studied. First, the effect of solution pH on the adsorption amount of L-Trp and L-Glu was studied. The adsorption selectivity and salt tolerance of the resin were investigated. Second, the adsorption mechanisms of L-Trp on the resin were illuminated by adsorption equilibria and a kinetics analysis. Finally the dynamic separation process of L-Trp was studied, and the separation effect was analyzed. This work can provide references for an efficient and clean separation of L-Trp and its analogues.

2. RESULTS AND DISCUSSION

2.1. Effect of pH on the Adsorption Amount of L-Trp and L-Glu. The adsorption amount of L-Trp and L-Glu on the resin HD-1 at different solution pH is shown in Figure 1. As can be seen from Figure 1, the adsorption amount of L-Trp increases first and then decreases as pH increases. The trend is similar to the concentration distribution of L-Trp$^{\pm}$ at different pH values (see Figure 2. The value of the dissociation equilibrium constant for L-Trp is $10^{-2.38}$ and $10^{-9.39}$). The result indicates that L-Trp$^{\pm}$ is the most favorable form for L-Trp adsorption. The resin HD-1 can adsorb L-Trp$^{\pm}$ based on hydrophobic interaction between the indolyl in L-Trp molecules and resin skeleton. The value of pK_a of the carboxyl groups on resin HD-1 is ∼3.15, which is calculated by the method developed by Tao et al.[19] When the solution pH is lower than 2.0, the adsorption amount of L-Trp decreases as pH decreases. In the pH range, the concentration ratio of L-Trp^{+} increases as pH decreases (see Figure 2). The carboxyl groups on the resin do not dissociate. The larger solubility of L-Trp^{+} in its aqueous solution than that of L-Trp$^{\pm}$ is unfavorable for the adsorption of L-Trp^{+}. Therefore, the adsorption amount of L-Trp decreases as pH decreases. When the solution pH is higher than 6.0, the adsorption amount of L-Trp decreases as pH increases. The degree of dissociation of carboxyl groups on the resin and the concentration ratio of L-Trp^{-} increases as pH increases. The electrostatic repulsion between L-Trp^{-} and dissociated carboxyl groups reduces the adsorption amount of L-Trp.

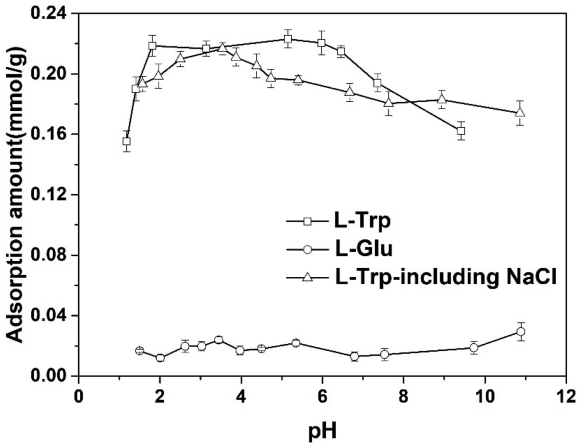

Figure 1. Adsorption amount of L-Trp and L-Glu on the resin HD-1 at different pH values.

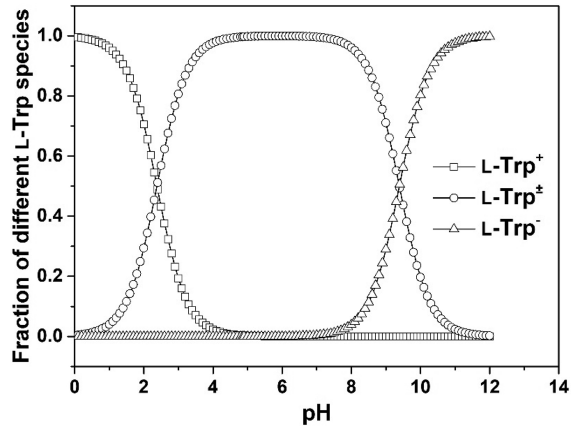

Figure 2. Concentration fraction of different species of L-Trp at different pHs.

In the pH range of 1.5−11, the adsorption amount of L-Trp is significantly higher than that of L-Glu (see Figure 1). The result indicates that the resin HD-1 shows a high adsorption selectivity to L-Trp. The high adsorption selectivity benefits the separation of L-Trp. The isoelectric point of L-Glu is ∼3.22.[20] When the solution pH is lower than 3.22 and higher than 3.15, L-Glu possesses a positive charge. Some carboxyl groups on resin HD-1 dissociate and become negatively charged.

https://doi.org/10.1021/acsomega.1c06960
ACS Omega 2022, 7, 9614−9621

However, the ratio of L-Glu$^+$ and the degree of dissociation of the resin are not high. Therefore, few L-Glu molecules are adsorbed on the resin in the pH range. When the solution pH is lower than 3.15, most of the L-Glu molecules carry a positive charge. A few carboxyl groups on the resin dissociate. There are no strongly hydrophobic groups in L-Glu molecules. Therefore, the adsorption amount of L-Glu is very low. When the solution pH is higher than 3.22, L-Glu molecules carry a negative charge. L-Glu is hard to be adsorbed by the resin whether or not the carboxyl groups on resin HD-1 dissociate. Therefore, the very low adsorption amount of L-Glu is reasonable in the pH range of 1.5−11.

When NaCl exists in the solution, the adsorption amount of L-Trp decreases slightly in the pH range of 2−8.5 (see Figure 1). NaCl can destroy the hydrogen bonds.[21] The decrease of the adsorption amount of L-Trp is probably due to the hydrogen bonds between L-Trp molecules, and the hydroxyl groups on the resin are destroyed by NaCl. When the pH is higher than 8.5, NaCl promotes the adsorption of L-Trp. Electrostatic repulsion exists between L-Trp molecules and the resin at those pHs. The electrostatic repulsion can be weakened by NaCl due to an electrostatic shielding effect.[22] Therefore, the adsorption amount of L-Trp increases slightly. In summary, the resin presents a high adsorption selectivity to L-Trp and excellent resistance to soluble salts.

2.2. Adsorption Equilibria of L-Trp on the Resin HD-1.

The adsorption isotherms of L-Trp at different pH values are shown in Figure 3. The adsorption amounts of L-Trp at pH 3, 4, and 5 are all higher than those at pH 1.5 and 9.5 at the same equilibrium concentration of L-Trp. The results are consistent to those shown in Figure 1. The adsorption isotherm data are fitted by Langmuir and Freundlich adsorption isotherm models, respectively, using the nonlinear fitting in Origin 9.1. The model parameters are listed in Table 1. As can be seen from Table 1, the values of the correlation coefficient R^2 for the Freundlich isotherm model are all higher than those for the Langmuir isotherm model. This result indicates that the adsorption isotherms of L-Trp fit to Freundlich isotherm model well. The values of n at different pHs are all larger than 1.0. The result indicates that there are heterogeneous adsorption sites on resin HD-1 and that various interactions including a hydrophobic interaction, hydrogen bonding, and electrostatic interaction play a role in the adsorption process of L-Trp.[23,24] The values of K_F first increase and then decrease as pH increases. The trend in the change of K_F is identical to that of the adsorption amount of L-Trp (see Figure 1). The result is rational because K_F indicates the adsorption amount of adsorbates. The larger the values of K_F are, the larger the adsorption amount is.[25]

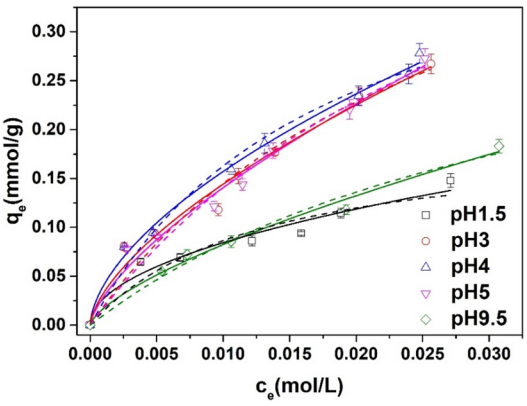

Figure 3. Adsorption isotherms of L-Trp at different pHs. Full and dash lines are fitting curves by Freundlich and Langmuir adsorption isotherm models, respectively.

Table 1. Adsorption Isotherm Model Parameters of L-Trp

	Langmuir model			Freundlich model		
pH	q_m (mmol/g)	K_L (L/mol)	R^2	K_F (mmol$^{1-1/n}$L$^{1/n}$/g)	n	R^2
1.5	0.20	79.47	0.914	0.82	2.02	0.958
3	0.54	36.56	0.957	2.79	1.55	0.977
4	0.45	55.78	0.984	2.37	1.70	0.995
5	0.62	29.17	0.968	3.36	1.45	0.984
9.5	0.39	27.36	0.976	1.93	1.46	0.988

The adsorption isotherm data of L-Trp at pH 1.5, 4, and 9.5 are fitted by the Dubinin−Radushkevich model. The fitting results are shown in Figure 4. The adsorption energy for L-Trp at pH 1.5, 4, and 9.5, which is calculated by the slope of fitting curves, is 6.90, 7.24, and 6.40 kJ/mol, respectively. The adsorption energy is lower than 8.0 kJ/mol. This result indicates that L-Trp molecules are adsorbed by resin HD-1 mainly based on non-electrostatic interactions.[22] The electrostatic interaction is a supplement for L-Trp adsorption due to the adsorption energy approaching to 8.0 kJ/mol.

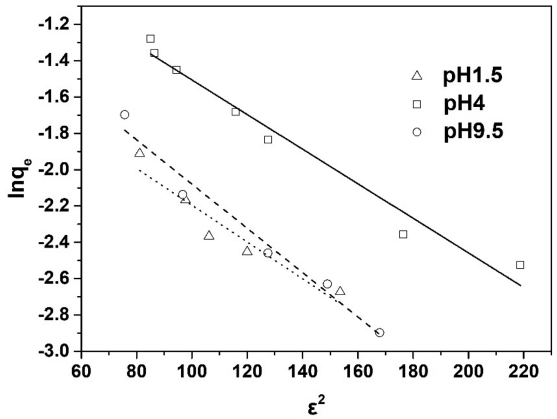

Figure 4. Adsorption isotherms fitted by Dubinin−Radushkevich model. Full, dash, and dot lines are the fitting curves at pH 4.0, 9.5, and 1.5, respectively.

Fixed-bed is the most common operation mode for the chromatographic separation technique. The simulation of the concentrations of L-Trp and pH in the fixed-bed can provide significant guidance for the optimization of operating conditions. During the column dynamic separation process of L-Trp, the pH of the mobile phase in the fixed-bed varies with the axial position. The adsorption of L-Trp depends on the solution pH. The adsorption isotherm model suitable for different pH is one of the necessary conditions for the establishment of an accurate fixed-bed separation process model.

L-Trp exists in the forms of cation, anion, and zwitterion in solution, and sometimes different forms of L-Trp coexist in solution. Different species of L-Trp interact with resin HD-1 in different ways. Physical adsorption of L-Trp$^{\pm}$ and L-Trp$^-$ occurs on the resin. L-Trp$^+$ reacts with resin HD-1 through ion exchange and physical adsorption. Resin HD-1 has a

https://doi.org/10.1021/acsomega.1c06960
ACS Omega 2022, 7, 9614−9621

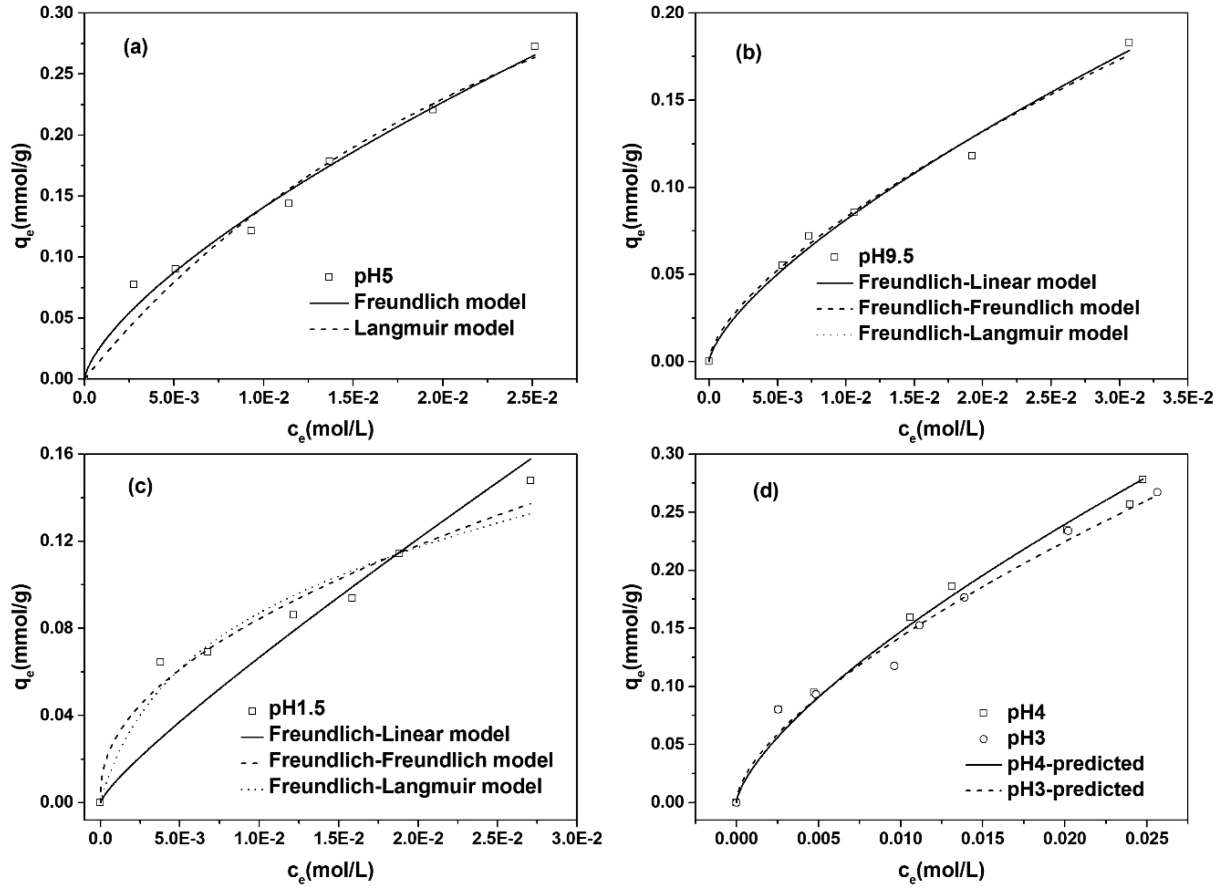

Figure 5. Experimental adsorption isotherm data and fitting curves of L-Trp at different pH values. (a) pH 5. (b) pH 9.5. (c) pH 1.5. (d) pH 3 and 4.

Table 2. Adsorption Isotherm Model Parameters for Different Species of L-Trp

	Langmuir model			Freundlich model		Linear model		
	q_m (mmol/g)	K_L (L/mol)	R^2	K_F (mmol$^{1-1/n}$L$^{1/n}$/g)	n	R^2	H	R^2
L-Trp$^{\pm}$	0.62	29.40	0.943	3.35	1.45	0.972	11.76	0.966
L-Trp^{-}	97.96	4.27×10^{-3}	0.988	0.01	5.38	0.988	0.42	0.990
L-Trp^{+}	0.08	234.60	0.941	0.27	2.89	0.962	3.96	0.855

weakly dissociated carboxyl group, and the degree of dissociation depends on the pH of the solution. The resins in different dissociation states have different ways of interacting with L-Trp. At pH 5.0, most of the L-Trp molecules exist as zwitterions. The adsorption isotherm data of L-Trp$^{\pm}$ were fitted to the Freundlich isotherm model, Langmuir isotherm model, and linear isotherm model, respectively. The fitting results are shown in Figure 5a and Table 2. By comparing the values of the correlation coefficient R^2, it is found that the Freundlich model can fit the adsorption isotherm data of L-Trp$^{\pm}$ well.

At pH 9.5, L-Trp exists as zwitterions and anions. The Freundlich(L-Trp$^{\pm}$)-linear(L-Trp^{-}) adsorption isotherm model, Freundlich(L-Trp$^{\pm}$)-Freundlich(L-Trp^{-}) adsorption isotherm model, and Freundlich(L-Trp$^{\pm}$)-Langmuir(L-Trp^{-}) adsorption isotherm model were used to fit the adsorption isotherm data at pH 9.5. The fitting results were shown in Figure 5b and Table 2. By comparing the values of the correlation coefficient R^2, it was found that the Freundlich-linear adsorption isotherm model could accurately fit the adsorption isotherm data at pH 9.5. The result indicates that the adsorption of L-Trp^{-} on resin HD-1 conforms to the linear relationship. At pH 1.5, L-Trp exists in the forms of zwitterion and cation. The carboxyl groups on resin HD-1 do not dissociate at pH 1.5. The Freundlich(L-Trp$^{\pm}$)-linear(L-Trp^{+}) adsorption isotherm model, Freundlich(L-Trp$^{\pm}$)-Freundlich (L-Trp^{+}) adsorption isotherm model, and Freundlich(L-Trp$^{\pm}$)-Langmuir(L-Trp^{+}) adsorption isotherm model were used to fit the adsorption isotherm data at pH 1.5. The fitting results were shown in Figure 5c and Table 2. By comparing the values of the correlation coefficient R^2, it was found that the Freundlich-Freundlich adsorption isotherm model could well fit the adsorption isotherm data at pH 1.5, indicating that the adsorption equilibrium relationship of L-Trp^{+} on the undissociated resin was in line with Freundlich adsorption isotherm model.

At pH 3.0 and 4.0, L-Trp exists in the forms of zwitterion and cation. The carboxyl groups on resin HD-1 dissociate. The Freundlich(L-Trp$^{\pm}$)-Freundlich(L-Trp^{+}) adsorption isotherm model-ideal mass action law(L-Trp^{+})[26] was used to fit the adsorption isotherm data at pH 3.0 and 4.0, respectively. The fitting results were found to be satisfactory (see Figure 5d). This result indicates that L-Trp^{+} reacts with resin HD-1 by

https://doi.org/10.1021/acsomega.1c06960
ACS Omega 2022, 7, 9614−9621

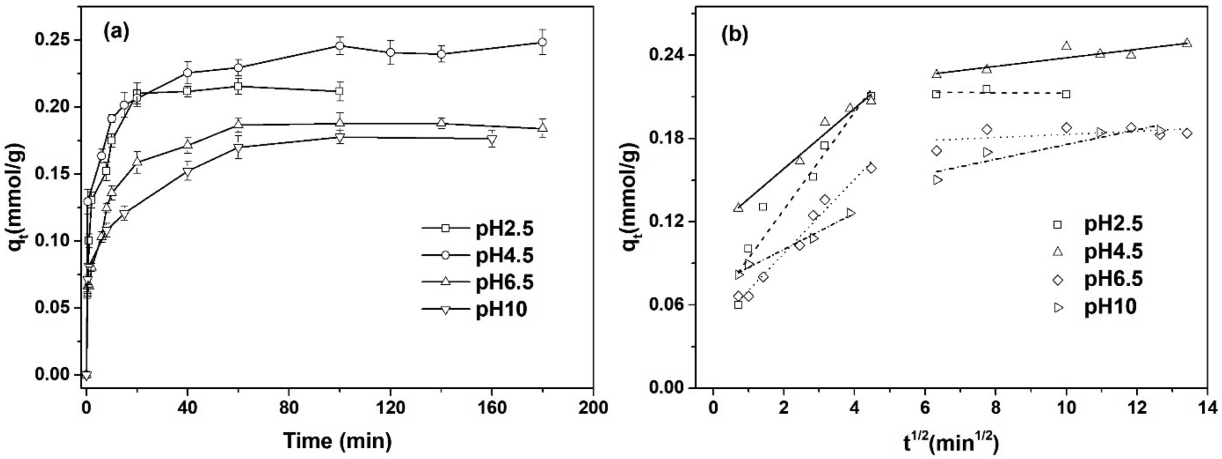

Figure 6. (a) Adsorption kinetic curves of L-Trp and (b) fitting curves by intraparticle diffusion model at different pHs.

physical adsorption and ion exchange. The adsorption isotherm model depending on solution pH can be expressed by the following formula.

$$q_e = f(c_{Trp^+}) + f(c_{Trp^\pm}) + f(c_{Trp^-}) \quad (1)$$

$$f(c_{Trp^+}) = K_F {c_{Trp^+}}^{1/n} + \alpha \frac{4Kc_{Trp^+}}{c_{H^+} + Kc_{Trp^+}} \quad (2)$$

$$f(c_{Trp^\pm}) = K_F {c_{Trp^\pm}}^{1/n} \quad (3)$$

$$f(c_{Trp^-}) = Hc_{Trp^-} \quad (4)$$

The values of $c_{Trp}{}^+$, $c_{Trp}{}^\pm$, and $c_{Trp}{}^-$ can be calculated by the total concentration of L-Trp and solution pH.[10] The degree of dissociation of the resin was calculated by the following equation.

$$\alpha = \frac{10^{-3.15}}{10^{-3.15} + 10^{-pH}} \quad (5)$$

2.3. Adsorption Kinetics of L-Trp on the Resin HD-1. The adsorption kinetic curves of L-Trp at different pHs are shown in Figure 6a. As can be seen from Figure 6a, the time required for L-Trp to reach adsorption equilibrium at pH 6.5 and 10 is longer than that at pH 2.5 and 4.5. At pH 6.5 and 10, the electrostatic repulsion between L-Trp and the resin leads to greater diffusion resistance of L-Trp molecules in the resin pores and a slower adsorption speed. The intraparticle diffusion model was used to fit the adsorption kinetics data. The fitting results were shown in Figure 6b. As can be seen from Figure 6b, the adsorption kinetics data under different pHs are divided into two linear regions. The first linear region did not pass the origin, indicating that the diffusion inside the particle and the liquid film together limited the mass transfer rate of L-Trp in the resin particles.[27]

2.4. Dynamic Separation Process of L-Trp in the Fixed-Bed Packed with Resin HD-1. The concentration profiles of L-Trp and L-Glu at the exit of the fixed-bed are shown in Figure 7. As can be seen from Figure 7, L-Glu flows out from the chromatographic column earlier than L-Trp. The phenomenon is due to the affinity between L-Glu and resin HD-1 being significantly weaker than that between L-Trp and resin HD-1. L-Trp and L-Glu were separated well with the purity of L-Trp higher than 99%, yield higher than 95%, the concentration ~4.69 × 10^{-3} mol/L, and eluent consumption

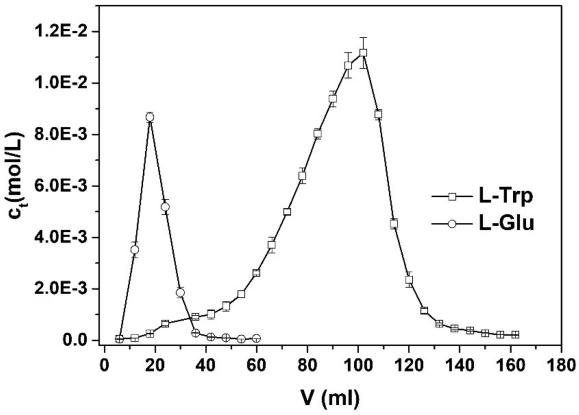

Figure 7. Concentration histories of L-Trp and L-Glu at the outlet of the fixed-bed.

of ~7.6 times that of the bed column. The productivity of L-Trp was 10.23 mmol/h/(g resin). In the adsorption process, L-Trp was adsorbed by the resin based on physical adsorption and ion exchange. In the elution process, there was electrostatic repulsion between L-Trp and the resin. Therefore, L-Trp flows out from the fixed bed quickly, so that the L-Trp chromatographic peak does not trail obviously. Resin HD-1 in the fixed-bed can be regenerated completely by ~60 mL of 0.5 mol/L HCl, and the separation performances of the resin have almost no change after being regenerated 10 times.

3. CONCLUSION

L-Trp was separated by physical adsorption and ion exchange mixed mode resin HD-1. The adsorption equilibria, kinetics, and column dynamics of L-Trp were studied. The resin has a high adsorption selectivity for L-Trp and excellent salt resistance. Various groups on the resin surface are involved in the adsorption process. The adsorption of L-Trp is mainly based on non-electrostatic interactions with the electrostatic repulsion as a supplement. The pH-dependent adsorption isotherm model proposed in this work can well fit the adsorption isotherm data under different pHs. The mass transfer rate of L-Trp is controlled by both the diffusion in particles and that in the liquid film at the outer surface of the particles. The fixed-bed packed with resin HD-1 can separate L-Trp well. The purity of the L-Trp product is higher than 99%, and the yield is higher than 95%. In our future work, the

https://doi.org/10.1021/acsomega.1c06960
ACS Omega 2022, 7, 9614−9621

continuous separation process will be studied to further improve the separation efficiency of L-Trp. The batch adsorption kinetic model and dynamic separation process model combining ion exchange and physical adsorption will be developed to optimize the separation process of L-Trp. In sum, this work can provide researchers a basis and reference for the efficient separation and purification of L-Trp and its analogues.

4. MATERIALS AND METHODS

4.1. Resin. The resin HD-1 was purchased from Sunresin New Materials Co. Ltd. The physicochemical properties of the resin were listed in Table 3. The resin was soaked in 0.5 mol/L NaOH aqueous solution for more than 4 h and then washed by deionized water until the solution pH approached 10.0. The resin was subsequently soaked in 0.5 mol/L HCl aqueous solution for more than 4 h. Then the resin was washed by deionized water until the solution pH approached 5.0.

Table 3. Physicochemical Properties of the Resin HD-1

properties	
skeleton	phenolic condensation framework
functional group	carboxyl
total ion exchange capacity (mmol/g)	4.0
moisture content	69.02%
wet apparent density (g/mL)	0.60−0.70

4.2. Chemicals. L-Trp (purity >99%), L-Glu (purity >99%), NaCl (purity >99.5%), sodium acetate (purity ≥99%), $K_2HPO_4{\cdot}3H_2O$ (purity ≥99%), acetic acid (purity ≥99.5%), 2,4-dinitrofluorobenzene (purity ≥98%), and $NaHCO_3$ (purity ≥99.8%) were all provided by Shanghai Macklin Biochemical Co., Ltd. NaOH (purity >96%) was obtained from Tianjin Jinbei Fine Chemical Co., Ltd. HCl (36%−38%, w/w) was purchased from China Pingmei Shenma Group Kaifeng Dongda Chemical Co., Ltd. Acetonitrile (chromatographic grade) was provided by Tianjin Kemiou Chemical Reagent Co., Ltd.

4.3. Analytical Methods. The concentration of L-Trp in the aqueous solutions was determined by ultraviolet−visible spectrophotometry (BioSpectrometer, Eppendorf AG) at 218 nm. The solution pH was determined by a pH meter (FE28, Mettler Toledo International Co., Ltd.). The concentration of L-Glu was analyzed by high-performance liquid chromatography (HPLC) (LC-20AT, Shimadzu Corporation) with a C18 column (250 × 4.6 mm, 5 μm, Shimadzu Corporation). The operating process for L-Glu analysis can be found in the literature.[17]

4.4. Effect of pH on the Adsorption Amount of L-Trp and L-Glu. An L-Trp aqueous solution (25 mL) at the concentration of ∼0.034 mol/L was settled into several Erlenmeyer flasks. The solution was adjusted to different pHs by adding HCl or NaOH aqueous solutions. Then 2 g of wet resin HD-1 was added into the flasks. The flasks were shaken at 150 rpm in a constant temperature shaker (298 ± 1 K) for more than 8 h to attain adsorption equilibrium. The pH and the concentration of L-Trp in the aqueous solution were measured. The adsorption amount of L-Trp was calculated by eq 6.

$$q_e = \frac{(c_0 - c_e)V}{m} \tag{6}$$

After a pretreatment that involved the removal of protein and pigments, the main soluble salts in the fermentation broth of L-Trp were mainly NaCl and NH_4SO_4. The total concentration of soluble salts is ∼0.63 mol/L. NaCl was selected as the representative soluble salt. The L-Trp aqueous solution containing 0.63 mol/L NaCl was used as the feed solution. The salt resistance of resin HD-1 was determined using identical operating steps to those of the aforementioned adsorption equilibrium experiments.

The adsorption amount of L-Glu at different pHs was measured using an identical method to that of L-Trp. The initial concentration of L-Glu is ∼9.52×10^{-3} mol/L.

4.5. Determination of Adsorption Isotherms of L-Trp. Different concentrations of an L-Trp aqueous solution (25 mL) were settled into several Erlenmeyer flasks. Then 2 g of wet resin HD-1 was added into the flasks. The pH of the aqueous solutions was adjusted to 1.5 by adding 0.1 mol/L HCl aqueous solution. Operating steps identical to those of Section 4.4 were used to measure the adsorption amount of L-Trp. The change curves of the adsorption amount of L-Trp under different equilibrium concentrations of L-Trp in its aqueous solutions are the adsorption isotherm at pH 1.5. Then the adsorption isotherms at pH 3, 4, 5, and 9.5 were determined, respectively, using the same operating steps as for the adsorption isotherm experiments at pH 1.5.

4.6. Adsorption Kinetic Experiments of L-Trp. Approximately 250 mL of an L-Trp aqueous solution (initial concentration of 0.034 mol/L) was adjusted to pH 2.5 by adding 0.1 mol/L HCl aqueous solution and then adding this into a round-bottom flask (500 mL). Ten grams of wet resin HD-1 was added into the flask. The solution was stirred intensely by a blender with a paddle. Then several samples were taken at predetermined moments to determine the concentration of L-Trp. eq 6 was used to calculate the adsorption amount of L-Trp at different times. The adsorption kinetic curve at pH 2.5 was drawn with the adsorption capacities at different times as ordinate and time as abscissa. Then the adsorption kinetic curves at pH 4.5, 6.5, and 10 were determined, respectively, using the same operating steps as at pH 2.5.

4.7. Dynamic Separation Experiments of L-Trp. Approximately 10 g of wet resin HD-1 was loaded into a glass column of inner diameter 1.15. An aqueous solution of HCl at pH 2.5 was introduced into the top of the column to wash the resin until the pH at the outlet of the column approached 2.5. Then the mixed solution of L-Trp (0.059 mol/L), L-Glu (9.52×10^{-3} mol/L), and NaCl (0.63 mol/L) at pH 2.5 was loaded into the top of the column. The concentrations of the mixed solution were selected based on the composition of the pretreated fermentation broth. The flow rate was kept at 0.3 mL/min by a peristaltic pump (BT100-1 L). After 13 mL of feed solution was loaded completely, 0.1 mol/L NaOH aqueous solution was used to elute the column. Several samples were taken at the outlet of the column at predetermined time intervals to determine the concentrations of adsorbates. The concentration of L-Glu was measured using HPLC. The product yield of L-Trp is the ratio of the mass of L-Trp in the collected product to that in the feed solution. The purity of L-Trp is determined by HPLC using identical operating procedures as for L-Glu.

https://doi.org/10.1021/acsomega.1c06960
ACS Omega 2022, 7, 9614−9621

5. THEORY

5.1. Adsorption Isotherm Models. Langmuir and Freundlich adsorption isotherm model equations are represented by eq 7 and eq 8, respectively.[28,29]

$$q_e = \frac{K_L c_e q_m}{1 + K_L c_e} \quad (7)$$

$$q_e = K_F {c_e}^{1/n} \quad (8)$$

The Henry adsorption isotherm model equation is as follows.

$$q_e = H c_e \quad (9)$$

The Dubinin−Radushkevich adsorption isotherm model equation is as follows.[22]

$$\ln q_e = \ln q_m - \varepsilon^2/(2{E_a}^2) \quad (10)$$

$$\varepsilon = RT \ln(1 + 1/c_e) \quad (11)$$

5.2. Intraparticle Diffusion Model. The intraparticle diffusion model equation proposed by Weber and Morris[30] can be described by eq 12.

$$q_t = k_p \times t^{1/2} + c \quad (12)$$

AUTHOR INFORMATION

Corresponding Author

Pengfei Jiao − *Research Center of Henan Provincial Agricultural Biomass Resource Engineering and Technology, College of Life Science and Agricultural Engineering, Nanyang Normal University, Nanyang 473061 Henan, China;* orcid.org/0000-0001-6918-2162; Phone: +86-0377-63513605; Email: jiaopf126@126.com; Fax: +86-0377-63512517

Authors

Xin Zhang − *Research Center of Henan Provincial Agricultural Biomass Resource Engineering and Technology, College of Life Science and Agricultural Engineering, Nanyang Normal University, Nanyang 473061 Henan, China*

Yuping Wei − *Research Center of Henan Provincial Agricultural Biomass Resource Engineering and Technology, College of Life Science and Agricultural Engineering, Nanyang Normal University, Nanyang 473061 Henan, China;* orcid.org/0000-0002-0069-3906

Yiyan Meng − *Research Center of Henan Provincial Agricultural Biomass Resource Engineering and Technology, College of Life Science and Agricultural Engineering, Nanyang Normal University, Nanyang 473061 Henan, China*

Complete contact information is available at: https://pubs.acs.org/10.1021/acsomega.1c06960

Notes

The authors declare no competing financial interest.

ACKNOWLEDGMENTS

This work was supported by the Scientific and Technological Project of Henan Province (Grant Nos. 202102110285 and 212102310868), School-level Research Project of Nanyang Normal University (Grant No. 2018ZX009), and National Innovation and Entrepreneurship Training Program for College Students (202110481004).

ABBREVIATIONS

c_0, Initial concentration, mol/L; c_e, Equilibrium concentration, mol/L; c, Constant; E_a, Adsorption energy, kJ/mol; H, Henry constant; K, Ion exchange equilibrium constant; K_F, Freundlich adsorption isotherm model constant, $mmol^{1-1/n}\ L^{1/n}/g$; K_L, Adsorption equilibrium constant, L/mol; k_p, Diffusion rate constant, $(mmol/g)/min^{1/2}$; m, Resin mass, g; n, Freundlich adsorption isotherm model constant; q_e, Equilibrium adsorption amount, mmol/g; q_m, Maximum monolayer adsorption capacity, mmol/g; q_t, Adsorption capacity at time t, mmol/g; R, Universal gas constant, J/mol·K; T, Absolute temperature, K; V, Volume of solution, mL; α, Degree of dissociation of the resin; ε, Effective adsorption potential energy, kJ/mol

Subscript

0, Before the adsorption; a, Adsorption; e, Adsorption equilibrium; F, Freundlich adsorption isotherm model; L, Langmuir adsorption isotherm model; m, Maximal; p, Particle; t, Time, min

REFERENCES

(1) Xu, Q.; Bai, F.; Chen, N.; Bai, G. Utilization of acid hydrolysate of recovered bacterial cell as a novel organic nitrogen source for L-tryptophan fermentation. *Bioengineered* **2019**, *10* (1), 23−32.

(2) Minliang, C.; Chengwei, M.; Lin, C.; Zeng, A.-P. Integrated laboratory evolution and rational engineering of GalP/Glk-dependent Escherichia coli for higher yield and productivity of L-tryptophan biosynthesis. *Metab Eng. Commun.* **2021**, *12*, 1−12.

(3) Niu, H.; Li, R.; Liang, Q.; Qi, Q.; Li, Q.; Gu, P. Metabolic engineering for improving L-tryptophan production in Escherichia coli. *J. Ind. Microbiol Biot* **2019**, *46*, 55−65.

(4) Chen, R.-Q.; Liu, W.; Pi, X.; Wang, X. The Research Progress of L-tryptophan. *J. Anhui Agr Sci.* **2014**, *42* (14), 4438−4440.

(5) Ikeda, M. Amino acid production processes. *Adv. Biochem Eng. Biotechnol* **2003**, *79*, 1−35.

(6) Chen, L.; Zeng, A. Rational design and metabolic analysis of Escherichia coli for effective production of L-tryptophan at high concentration. *Appl. Microbiol. Biotechnol.* **2017**, *101* (2), 559−568.

(7) Zhao, C.; Fang, H.; Wang, J.; Zhang, S.; Zhao, X.; Li, Z.; Lin, C.; Shen, Z.; Cheng, L. Application of fermentation process control to increase l-tryptophan production in Escherichia coli. *Biotechnol. Prog.* **2020**, *36* (2), No. e2944.

(8) Zhao, Z. J.; Zou, C.; Zhu, Y.-X.; Dai, J.; Chen, S.; Wu, D.; Wu, J.; Chen, J. Development of L-tryptophan production strains by defined genetic modification in Escherichia coli. *J. Ind. Microbiol Biot* **2011**, *38* (12), 1921−1929.

(9) Xiong, B.; Zhu, Y.; Tian, D.; Jiang, S.; Fan, X.; Ma, Q.; Wu, H.; Xie, X. Flux redistribution of central carbon metabolism for efficient production of L-tryptophan in Escherichia coli. *Biotechnol. Bioeng.* **2021**, *118* (3), 1393−1404.

(10) Jiao, P.; Zhang, X.; Li, N.; Wei, Y.; Wang, P.; Yang, P. Cooperative adsorption of L-tryptophan and sodium ion on a hyper-cross-linked resin: Experimental studies and mathematical modeling. *J. Chromatogr A* **2021**, *1648* (51), 462211−462219.

(11) Tan, B.; Luo, G.; Wang, J. Extractive separation of amino acid enantiomers with co-extractants of tartaric acid derivative and Aliquat-336. *Sep Purif Technol.* **2007**, *53* (3), 330−336.

(12) Saeki, M.; Shiroshita, Y.; Toyomasu, R. Method for crystallizing amino acid. *WO/1990/009372* **1990**, *08* (23), 1990.

(13) Liu, L.; Yang, L.; Jin, K.; Xu, D.; Gao, C. Recovery of L-tryptophan from crystallization wastewater by combined membrane process. *Sep Purif Technol.* **2009**, *66* (3), 443−449.

(14) Xie, Y.; Jing, K.; Lu, Y. Kinetics, equilibrium and thermodynamic studies of L-tryptophan adsorption using a cation exchange resin. *Chem. Eng. J.* **2011**, *171* (3), 1227−1233.
(15) Luo, W.; Wei, P.; Chen, H.; Fan, L.; Huang, L.; Huang, J.; Xu, Z.; Cen, P. Kinetics and optimization of L-tryptophan separation with ion-exchange chromatography. *Korean J. Chem. Eng.* **2011**, *28* (5), 1280−1285.
(16) Zhang, T.; Yang, S. Separation and purification of L-tryptophan from the fermentation broth rapidly. *Food Ind.* **2017**, *38* (2), 128−131.
(17) Jiao, P.; Wei, Y.; Zhang, M.; Zhang, X.; Zhang, H.; Yuan, X. Adsorption separation of L-tryptophan based on the hyper-cross-linked resin XDA-200. *ACS Omega* **2021**, *6* (3), 2255−2263.
(18) Halan, V.; Maity, S.; Bhambure, R.; Rathore, A. S. Multimodal chromatography for purification of biotherapeutics - A review. *Curr. Protein Pept Sci.* **2018**, *20* (1), 4−13.
(19) Zuyi, T.; Jinzhou, D.; Taiwei, C. Potentiometric titration in studies of ion exchangers. *React. Funct Polym.* **1996**, *31* (1), 17−24.
(20) Özdamar, T. H.; Takaç, S.; Çalik, G.; Ballica, R. Kinetics of ion exchange process for separation of glutamic acid. *Bioproc Biosyst Eng.* **1989**, *4* (6), 249−256.
(21) Lv, M. *Study on synthesis, characteristic and its application of Layered double hydroxide (Mg/Fe LDH);* Shanghai Ocean University: Shanghai, China, 2017.
(22) Wang, W.; Qi, M.; Jia, X.; Jin, J.; Zhou, Q.; Zhang, M.; Zhou, W.; Li, A. Differential adsorption of zwitterionic PPCPs by multifunctional resins: The influence of the hydrophobicity and electrostatic potential of PPCPs. *Chemosphere* **2020**, *241*, 125023.
(23) Wang, W.; Maimaiti, A.; Shi, H.; Wu, R.; Wang, R.; Li, Z.; Qi, D.; Yu, G.; Deng, S. Adsorption behavior and mechanism of emerging perfluoro-2-propoxypropanoic acid (GenX) on activated carbons and resins. *Chem. Eng. J.* **2019**, *364*, 132−138.
(24) Wang, W.; Deng, S.; Li, D.; Ren, L.; Shan, D.; Wang, B.; Huang, J.; Wang, Y.; Yu, G. Sorption behavior and mechanism of organophosphate flame retardants on activated carbons. *Chem. Eng. J.* **2018**, *332*, 286−292.
(25) Asante, B.; Sirviö, J. A.; Li, P.; Lavola, A.; Julkunen-Tiitto, R.; Haapala, A.; Liimatainen, H. Adsorption of bark derived polyphenols onto functionalized nanocellulose: Equilibrium modeling and kinetics. *AIChE J.* **2020**, *66* (2), 1−10.
(26) Jiao, P.; Wu, J.; Wang, Y.; Zhou, J.; Zhuang, W.; Chen, Y.; Liu, D.; Zhu, C.; Ying, H. Combined ion exchange and adsorption equilibria of 5′-ribonucleotides on the strong acid cation exchange resin NH-1. *J. Chem. Technol. Biot* **2017**, *92* (7), 1678−1689.
(27) Yang, S.; Gao, M.; Luo, Z.; Yang, Q. The characterization of organo-montmorillonite modified with a novel aromatic-containing gemini surfactant and its comparative adsorption for 2-naphthol and phenol. *Chem. Eng. J.* **2015**, *268*, 125−134.
(28) Burton, S. C.; Harding, D. R. K. Hydrophobic charge induction chromatography: salt independent protein adsorption and facile elution with aqueous buffers. *J. Chromatogr A* **1998**, *814* (1−2), 71−81.
(29) Hirano, A.; Maruyama, T.; Shiraki, K.; Arakawa, T.; Kameda, T. A study of the small-molecule system used to investigate the effect of arginine on antibody elution in hydrophobic charge-induction chromatography. *Protein Expres Purif* **2017**, *129*, 44−52.
(30) Weber, W. J.; Morris, J. C. Kinetics of adsorption on carbon from solution. *J. Sanit Eng. Div* **1963**, *89* (2), 1−2.

https://doi.org/10.1021/acsomega.1c06960
ACS Omega 2022, 7, 9614−9621